Available online at www.sciencedirect.com
ScienceDirect
Polymer 47 (2006) 7178–7188
polymer
www.elsevier.com/locate/polymer

Plasticization of semicrystalline poly(L-lactide) with poly(propylene glycol)

E. Piorkowska, Z. Kulinski, A. Galeski*, R. Masirek

Centre of Molecular and Macromolecular Studies, Polish Academy of Sciences, Sienkiewicza 112, 90 363 Lodz, Poland

Received 13 February 2006; accepted 24 March 2006
Available online 30 June 2006

To honor the memory of Tadeusz Pakula.

Abstract

Plasticization of semicrystalline poly(L-lactide) (PLA) with a new plasticizer – poly(propylene glycol) (PPG) is described. PLA was plasticized with PPG with nominal M_w of 425 g/mol (PPG4) and 1000 g/mol (PPG1) and crystallized. The plasticization decreased T_g, which was reflected in a lower yield stress and improved elongation at break. The crystallization in the blends was accompanied by a phase separation facilitated by an increase of plasticizer concentration in the amorphous phase and by annealing of blends at crystallization temperature. The ultimate properties of the blends with high plasticizer contents correlated with the acceleration of spherulite growth rate that reflected accumulation of plasticizer in front of growing spherulites causing weakness of interspherulitic boundaries. In PLA/PPG1 blends the phase separation was the most intense and led to the formation of PPG1 droplets, which facilitated plastic deformation of the blends and enabled to achieve the elongation at break of about 90–100% for 10 and 12.5 wt% PPG1 content in spite of relatively high T_g of PLA rich phase of the respective blends, 46.1–47.6 °C. Poly(ethylene glycol) (PEG), long known as a plasticizer for PLA, with nominal M_w of 600 g/mol, was also used to plasticize PLA for comparison.

Keywords: Poly(lactide); Poly(propylene glycol); Plasticization

1. Introduction

Poly(L-lactide) (PLA), a biodegradable polymer which can also be produced from annually renewable resources, is rigid and brittle below the glass transition temperature (T_g) which is in the range of 50–60 °C. Crystallinity, if developed, increases the modulus of elasticity and further decreases the drawability [1]. PLA has been plasticized to increase its ability to plastic deformation. Poly(3-methyl-1,4-dioxan-2-one) [2], poly(ethylene oxide) [3], citrate esters [4,5], triacetine [5] and poly(ethylene glycol)s (PEGs) [6–10] were found to be efficient plasticizers for PLA. The transition from brittle to ductile behaviour in the plasticized PLA occurs when T_g is decreased to 35 °C. The plasticization effect is enhanced by higher PEG content, however, blends of PLA with PEG undergo phase separation at a certain PEG content, depending on PEG molecular weight. One of the reasons of instability of PLA/PEG blends is crystallization of PEG that depletes the amorphous phase of the plasticizer [9,11].

Much less is known about the plasticizing effect of PEG on semicrystalline PLA. In studies devoted to the mechanical properties of plasticized PLA, its crystallization was rather a side effect that occurred at a relatively high plasticizer content, where PEG separation in the amorphous phase was also observed [12]. Recently, Kulinski and Piorkowska [10] have demonstrated that the cold crystallization in PLA plasticized with PEG decreases significantly its drawability. While an amorphous blend with 10 wt% of PEG with M_w about 600 g/mol can be drawn to more than 500%, only about 20% elongation at break was achieved for the same blend after cold crystallization.

An upper temperature limit of applicability of an amorphous polymer is determined by its T_g, while that of a semicrystalline polymer by its melting temperature, usually much higher. Thus, the plasticized semicrystalline PLA with improved drawability

* Corresponding author. Fax: +48 42 6819850.
E-mail address: andgal@bilbo.cbmm.lodz.pl (A. Galeski).

0032-3861/$ - see front matter © 2006 Elsevier Ltd. All rights reserved.
doi:10.1016/j.polymer.2006.03.115

would be an attractive material. Also the migration of plasticizer molecules to a material surface [13], worsening the material properties, should be limited in the semicrystalline material.

Recently, Kulinski et al. [14] reported plasticization of amorphous PLA with two poly(propylene glycol)s (PPGs) differing in molecular weight. PPGs are viscous liquids with molecular weight ranging 150–4000 g/mol and T_g of −60 to −75 °C [16]. According to Ref. [14] PPG with higher molecular weight separated from amorphous PLA when its content reached 12.5 wt%, but tiny liquid pools of PPG did not deteriorate the ability of the blend to plastic deformation.

In the present paper we describe the plasticization of semicrystalline PLA with the two PPGs differing in molecular weight and also with PEG, for comparison. It is demonstrated that both PPGs increased the ability of semicrystalline PLA to plastic deformation more efficiently than PEG. This finding was correlated with crystallization behaviour and structure of the blends.

2. Experimental

The study utilized poly(L-lactide) manufactured by Hycail BV (the Netherlands) (PLA), with residual lactide content of 0.5%, according to the producer, and M_w of 108 kg/mol, $M_w/M_n = 1.6$ as determined by a GPC method in methylene chloride. The specific optical rotation, $[\alpha]_D^{25}$, of this PLA was −136.7 as determined in methylene chloride at a concentration of 1 g/dl and at 25 °C using Perkin Elmer 241MC Polarimeter. The concentration of D-lactide was calculated as 6.2% assuming $[\alpha]_D^{25}$ of poly(L-lactide) and poly(D-lactide) to be −156 and +156, respectively [15]. This finding is confirmed by ^{13}C NMR spectrum, presented in Fig. 1, where a significant amount of tetrads iss and ssi is detected in the methine resonance range (PLA dissolved in $CDCl_3$, Bruker DRX500 500 MHz, ^{13}C). The significant amount of D-lactide distributed along PLA chains causes a decrease of ability of PLA to crystallize and a decrease of melting temperature to the range of 130–135 °C with the respect to that of 100% poly(L-lactide).

Two PPGs with nominal M_w equal to 425 g/mol (PPG4) and 1000 g/mol (PPG1), purchased from Sigma–Aldrich, were used as plasticizers. PEG with nominal M_w of 600 g/mol was also applied to plasticize PLA for comparison.

MALDI Time of Flight technique [10,14] enabled to establish that M_w and M_w/M_n were equal to 530 g/mol and 1.03 for PPG4, 1123 g/mol and 1.05 for PPG1 and 578 g/mol and 1.08 for PEG, respectively. These values are close to the respective values specified by suppliers. Molecular weight characteristics of PEG are also close to the corresponding values for PPG4, so activities of these plasticizers can be compared. T_g of PPG4 and PPG1, measured by a DSC method was −72 and −70 °C, respectively, while PEG melting peak was centered at +20 °C [14].

Prior to blending, the polymers were vacuum dried at 100 °C for 4 h. Melt-blends containing 5, 7.5, 10 and 12.5 wt% of plasticizers were prepared using a Brabender mixer operating at 190 °C for 20 min at 60 rpm, under the flow of dry gaseous nitrogen. Neat PLA was also processed in the same way in order to obtain a reference material. The blends will be referred throughout the paper as PLA/PPG4, PLA/PPG1 and PLA/PEG with a number indicating percentage of plasticizer, for instance: PLA/PPG4-5 for the blend of PLA with 5 wt% of PPG4.

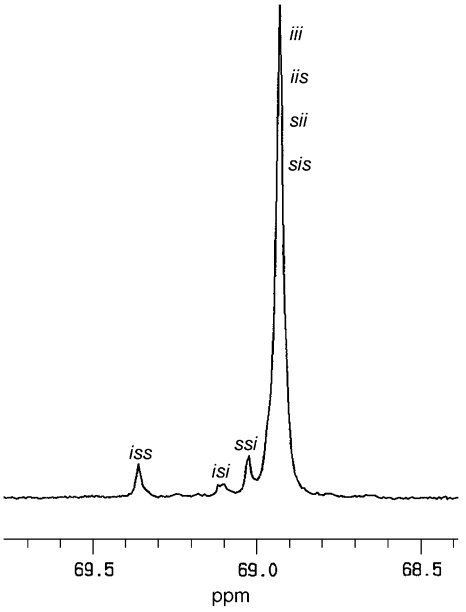

Fig. 1. ^{13}C NMR spectrum of PLA dissolved in $CDCl_3$ in the methine range. Tetrads are identified on the plot.

Cold crystallization was chosen as a crystallization method because it leads to more intense spherulite nucleation resulting in shorter crystallization time and smaller spherulite sizes [17]. Pre-crystallization thermal treatment and crystallization conditions for all the materials were based on preliminary studies involving differential scanning calorimetry (DSC), carried out with a TA Instrument 2920 DSC on 10–12 mg specimens of all materials.

Entirely amorphous films of 0.4–0.5 and 1 mm thick amorphous films of PLA and plasticized PLA were prepared by compression molding at 180 °C for 3 min followed by quenching between thick metal blocks kept at room temperature. Then, the films were cold-crystallized at 90 °C between two metal blocks equipped with heaters and Pt resistance thermometers connected to a temperature controller which enabled holding steady temperature with an accuracy of 0.2 K; other details of the method are given elsewhere [10]. Time required for crystallization varied from 45 min to 3 h depending on a material composition; the longest was for neat PLA while the shortest for PLA/PEG-12.5.

All materials and molded films were stored in dry atmosphere in desiccators at ambient temperature.

The films were characterized by the DSC technique at a heating rate of 10 K/min. T_g of all the materials was measured as the temperature corresponding to the midpoint of the heat capacity increment. In addition, the measurements at heating rate of 1 K/min, amplitude 0.106 K, and frequency 1/40 Hz were conducted for neat PLA and the blends in a TA Instruments Modulated DSC 2920 (MDSC). Dynamic mechanical thermal analysis (DMTA) and tensile measurements

were performed on specimens cut out from freshly molded and crystallized films one day before the tests. Dynamic mechanical properties of the materials were measured in the three point bending mode in a DMTA Mk III, Rheometric Scientific Ltd. apparatus at frequency of 1 Hz, during heating at the rate of 2 K/min, on rectangular samples, 14 mm × 32 mm, cut out from 1 mm thick films. Tensile tests were performed on an Instron machine at the rate of 0.5 mm/min, in a temperature chamber with circulating air, at 25 °C, on oar-shaped specimens, with 9.53 mm gauge length, and width of 3.18 mm cut out from 0.5 mm thick films.

The crystal structure of films was probed by a wide angle X-ray diffraction (WAXS) in the reflection mode while the long period was determined by 2-D small angle X-ray scattering (2-D SAXS). To determine an average spherulite size, a small angle light scattering (SALS) method was employed. X-ray and SALS measurements utilized the equipments and methods described in detail in Ref. [10]. For SALS measurements films of thickness approx. 60 μm were compression molded between microscope cover glasses and crystallized at 90 °C under the flow of gaseous nitrogen in a Linkam hot stage THMS 600 mounted in a light microscope, employing the same protocol for temperature control that was used for films for mechanical tests. The spherulite growth rate measurements during isothermal crystallization at 90 °C in Linkam hot stage utilized 10 μm thick films prepared using the procedure that was used for crystallization of films for SALS measurements.

Polarized light microscope, with crossed polarizers, was also employed to study the gauge regions of samples drawn to fracture. The fracture surfaces of all materials were studied under a Jeol 5500LV scanning electron microscope (SEM). To have an insight into blend morphology prior to deformation, 0.5 mm thick films of the crystallized blends were submerged in liquid nitrogen and broken to expose the internal structure for SEM studies. Prior to the SEM examination all surfaces were sputtered with gold.

3. Results

3.1. Structure and thermal properties

Exemplary heating thermograms of the films of PLA and plasticized PLA are shown in Fig. 2. T_g of blends was always lower than that of neat PLA. The plasticizer decreased T_g from about 56 °C for neat PLA to 38–41 and 34–39.5 for the blends with 5, and 7.5 wt% of plasticizers, respectively. The lower values of temperature ranges correspond to the glass transition temperatures of PLA/PPG4 and PLA/PEG, while the higher to those of PLA/PPG1. The efficiency of PPG4 and PEG in decreasing the glass transition temperature was similar, while PPG1 was less efficient. Glass transition in PLA/PPG4 and PLA/PEG blends with 10 and 12.5 wt% of plasticizers, beginning below room temperature, was very broad and diffused. The broadening of glass transition was also reflected in MDSC reversing heat flow, as it is shown in Fig. 3. Fig. 4 shows the low temperature part of the thermograms recorded for the blends

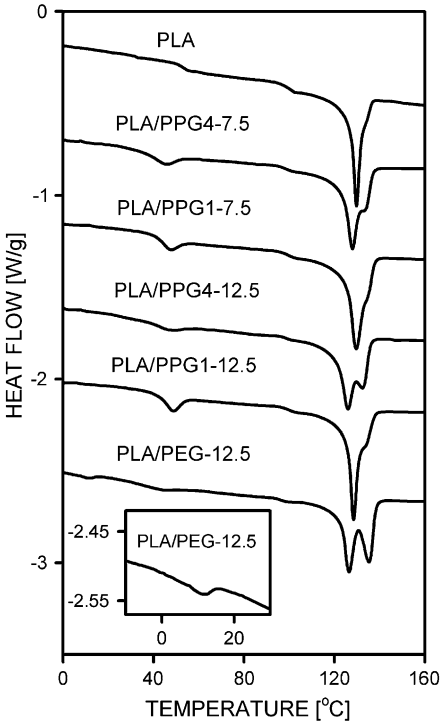

Fig. 2. Exemplary DSC heating thermograms recorded for PLA, PLA/PPG4, PLA/PPG1 and PLA/PEG blends. Thermograms shifted vertically.

with 12.5 wt% of plasticizer. Traces of weak and rather diffuse glass transitions at approx. −65 °C were discernible on the DSC thermograms of PLA/PEG-10 and PLA/PEG-12.5 blends. Very weak glass transition with T_g at −73 °C was also recognizable for PLA/PPG4-12.5 and at −78 °C for PLA/PPG1-7.5 and PLA/PPG1-10. In contrast, PLA/PPG1-12.5 blend exhibited more pronounced glass transition around −78 °C. In addition, very small melting peaks at 11 °C, as the one shown in the inset in Fig. 2, were also detected for PLA/PEG-10 and PLA/PEG-12.5 blends and attributed to melting of PEG crystals. However, the melting enthalpy, at the level of 0.2 and 0.4 J/g for the blends with 10 and 12.5 wt% of PEG, respectively, indicated that the melting crystals constituted only 0.14 and 0.27 wt% of the blends (assuming the enthalpy of fusion of 146.7 J/g for 100% crystalline PEG [18]).

The T_g values are lower than those measured for both pure PPGs by DSC at the same heating rate, especially in the case of PPG1, and also the melting temperature of PEG crystals is lower than that of pure PEG. The decrease of T_g of inclusions dispersed in glassy matrix was observed in the past for other systems and explained by others as a result of negative pressure developed during cooling due to thermal shrinkage mismatch of inclusions and matrix [19]. Also a decrease of equilibrium melting point due to negative pressure observed for polymers [20] explains the lowering of melting point of PEG. Coexistence of glass transition of PEG rich phase and melting of PEG crystals on the same thermograms suggests that only a fraction of PEG crystallized in the PEG rich phase upon cooling in the DSC.

Melting of PLA crystals began above 90 °C in all the materials. Single melting peak, centered at 130 °C was observed

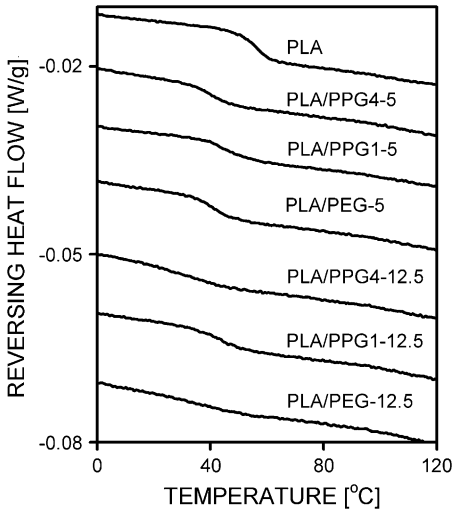

Fig. 3. Exemplary MDSC thermograms recorded for PLA, PLA/PPG4, PLA/PPG1 and PLA/PEG blends. Thermograms shifted vertically.

for neat PLA. In the blends, with the increase of the plasticizer content the melting peak shifted gradually to a lower temperature, at most to 126 °C for PLA/PPG4 and PLA/PEG and to 128 °C for PLA/PPG1. Exemplary 2θ scans for PLA and PLA plasticized with PPGs plotted in Fig. 5 reveal peaks typical of α-crystallographic form described as pseudo-orthorhombic [21] or orthorhombic [22].

On the thermograms of PLA/PPG1 blends a shoulder appeared on the descending slope of the melting peak at about 133 °C. For the PLA/PPG4 blends the shoulder developed into a second melting peak for the PPG4 content of 7.5 wt% and higher. For all the PLA/PEG blends high temperature melting peaks, higher than those recorded for PLA/PPG4 blends with a similar plasticizer content, were observed. The additional melting peaks on thermograms of plasticized PLA were already explained as related to the reorganization of crystal structure [3,10]. The reorganization was obviously more

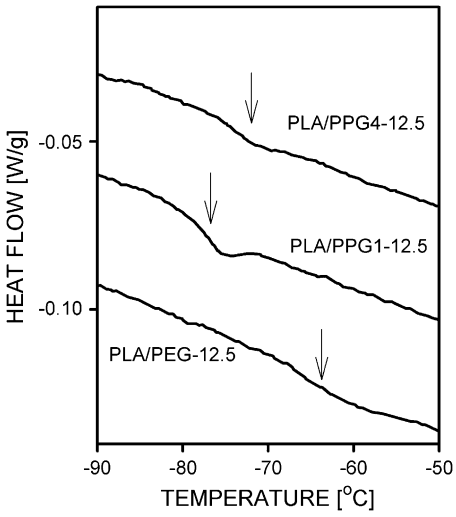

Fig. 4. Low temperature parts of DSC heating thermograms recorded for blends: PLA/PEG-12.5, PLA/PPG1-12.5 and PLA/PPG4-12.5. Thermograms shifted vertically.

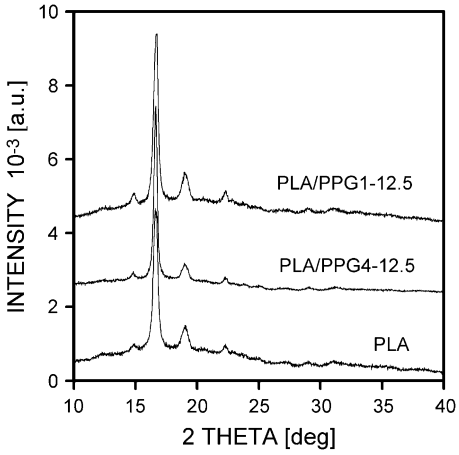

Fig. 5. X-ray diffractograms of neat PLA and blends: PLA/PPG4-12.5 and PLA/PPG1-12.5.

intense in PLA/PEG blends than in PLA/PPG blends indicating better stability of lamellae in the latter. The melting enthalpy, equal to 32 J/g for neat PLA and 30–32 J/g for the blends, corresponds to the crystallinity level of 29–30 wt% if the enthalpy of fusion of 106 J/g is assumed [23]. Similar long period values, 19–20 nm, were determined by the SAXS method for neat PLA and for the blends with 12.5 wt% of plasticizers. The crystallinity level in the blends is similar as in neat PLA thus the decrease of melting temperature of PLA crystals in the blends should be attributed to their less perfection, especially that PEG plasticizers are known to decrease the surface energy [24] which should increase crystal stability.

Temperature dependencies of the loss modulus E'' for neat and plasticized PLA are shown in Fig. 6. The log E'' peak temperatures exceeded the DSC T_g values by few degrees; it is known that 1 Hz DMTA data may correspond to a DSC heating rate in the range of 20–40 K/min [25], higher than used here (10 K/min). The log E'' glass transition peak temperature, 59 °C for neat PLA, is shifted to lower values in plasticized PLA, depending on the plasticizer type and its content (Fig. 7). Log E'' peak temperatures decreased with the increase of plasticizer content for all the blends although the dependence was the weakest in the case of the PLA/PPG1 blends. The peaks recorded for PLA/PPG4 and PLA/PEG blends, broadened with the increase of plasticizer content, although more for the PLA/PEG systems. Tan δ peak (not shown) also shifted to lower temperature for PLA/PPG4 and PLA/PEG blends with the increase of plasticizer content while for PLA/PPG1 blends it remained nearly at the same temperature as for neat PLA.

Crystallization of PLA exudes a plasticizer into the amorphous phase and increases its content by approx. 50%, thus a T_g decrease could be expected. Comparison of DMTA data of crystallized blends with those for the amorphous blends [14] shows that the temperature of E'' glass transition peak of PLA/PPG4 blends decreased after crystallization by approx. 2 K that is less than 5–6 K which could be anticipated based on the dependence of T_g on PEG4 content for the amorphous blends [14]. For PLA/PEG and PLA/PPG1 blends, the

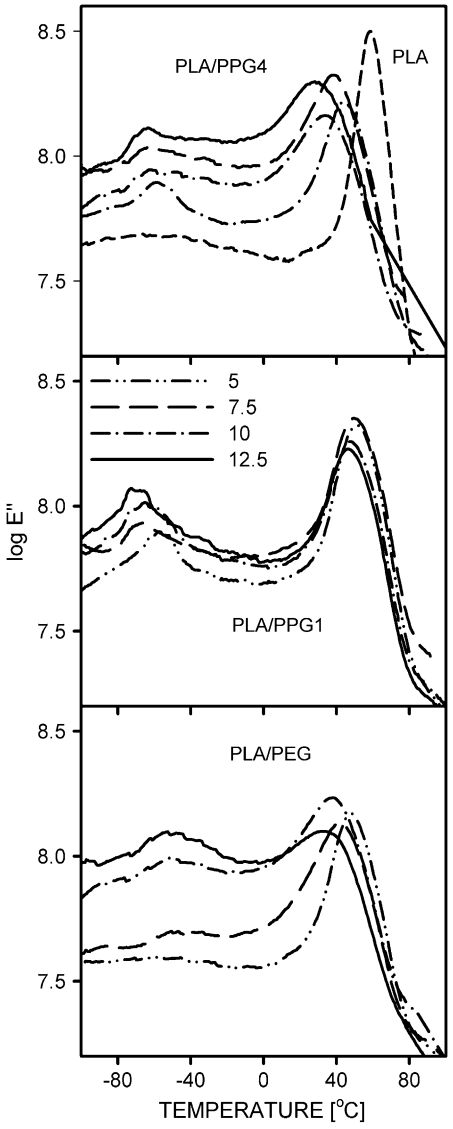

Fig. 6. Temperature dependence of log E'' for neat PLA and blends: PLA/PPG4, PLA/PPG1 and PLA/PEG with various plasticizer contents.

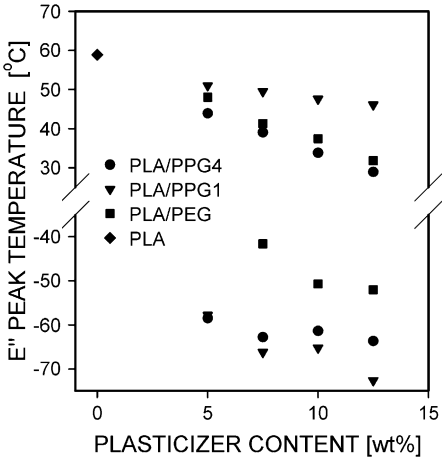

Fig. 7. Temperature of log E'' peaks for neat PLA and for PLA/PPG4, PLA/PPG1, PLA/PEG blends vs. plasticizer content.

temperature of log E'' glass transition peak increased after crystallization up to approx. 4 and 6.5 K, respectively; the increase was enhanced by a higher plasticizer content. In addition, the log E'' plots for the crystallized blends, especially those with high plasticizer contents, are featured by additional low temperature peaks, broad for PLA/PEG blends and sharper for PLA/PPG blends; the peak temperatures are plotted in Fig. 6. The low temperature peak of log E'' plot for a PLA/PEG blend was already observed by others and correlated with a formation of PEG rich phase [26]. Similarly, the low temperature peaks recorded for PLA/PPG blends can result only from a phase separation in the amorphous phase leading to the formation of a plasticizer rich phase and depleting the PLA of plasticizer. The phase separation in the amorphous phase was already reflected in additional low temperature glass transitions of the blends and in melting peaks of PEG crystals in PLA/PEG blends evidenced by the DSC measurements. The amorphous blends studied in Ref. [14] were homogeneous except for PLA/PPG1-12.5. In the present study the phase separation was obviously driven by an increase of a plasticizer content in the amorphous phase and was also facilitated by temperature and time required for crystallization.

Upon phase separation the PPG1 plasticizer accumulated in distinct pools. SEM studies of fracture surfaces of the films broken in liquid nitrogen revealed some emptied voids in PLA/PPG1 blends where PPG1 accumulated during phase separation (Fig. 8). In PLA/PPG1-5 the voids surround void free areas of sizes corresponding to the spherulite size as measured by the SALS method for this blend. An increase of PPG1 content to 7.5 wt% results in broadening of void inhabited zones while in PLA/PPG-10 and PLA/PPG1-12.5 a distribution of voids over the samples became uniform. Evidence of separate plasticizer inclusions was found by SEM neither in PLA/PPG4 nor in PLA/PEG blends.

An average spherulite radius, determined by a SALS method was 3.3 μm in PLA, 6–7.5 μm in PLA/PEG, 10.5–11.5 μm in PLA/PPG4 and 12.5–13.5 μm in PLA/PPG1 blends. Although all the plasticizers decreased the nucleation density, D, the effect induced by both PPGs was stronger than that of PEG. In the simplest case of instantaneous nucleation the conversion of melt into spherulites depends on DG^3, G being the spherulite growth rate. The decrease of D by 2^3–4^3 times in the blends was, however, compensated by an increase of G. All the plasticizers used increased the spherulite growth rate at 90 °C, G, by the factor of 3–24, which is illustrated in Fig. 9, although both PPGs enhanced the growth rate less than PEG. The faster growth rate and/or shorter time available for isothermal annealing of crystals facilitated probably the formation of less perfect crystals. G in the blends increased with the increase of plasticizer content with the exception of PLA/PPG1-12.5 for which G was nearly equal to that in PLA/PPG1-10. G in neat PLA and in all blend types with plasticizer contents of 5 and 7.5 wt% was stable with time. It was also stable in the sample PLA/PPG1-10. In other blends, with higher plasticizer contents the growth accelerated with time; most pronounced acceleration was observed in PLA/PEG-12.5. Exemplary dependencies of the radius of growing spherulites on time are plotted in Fig. 10.

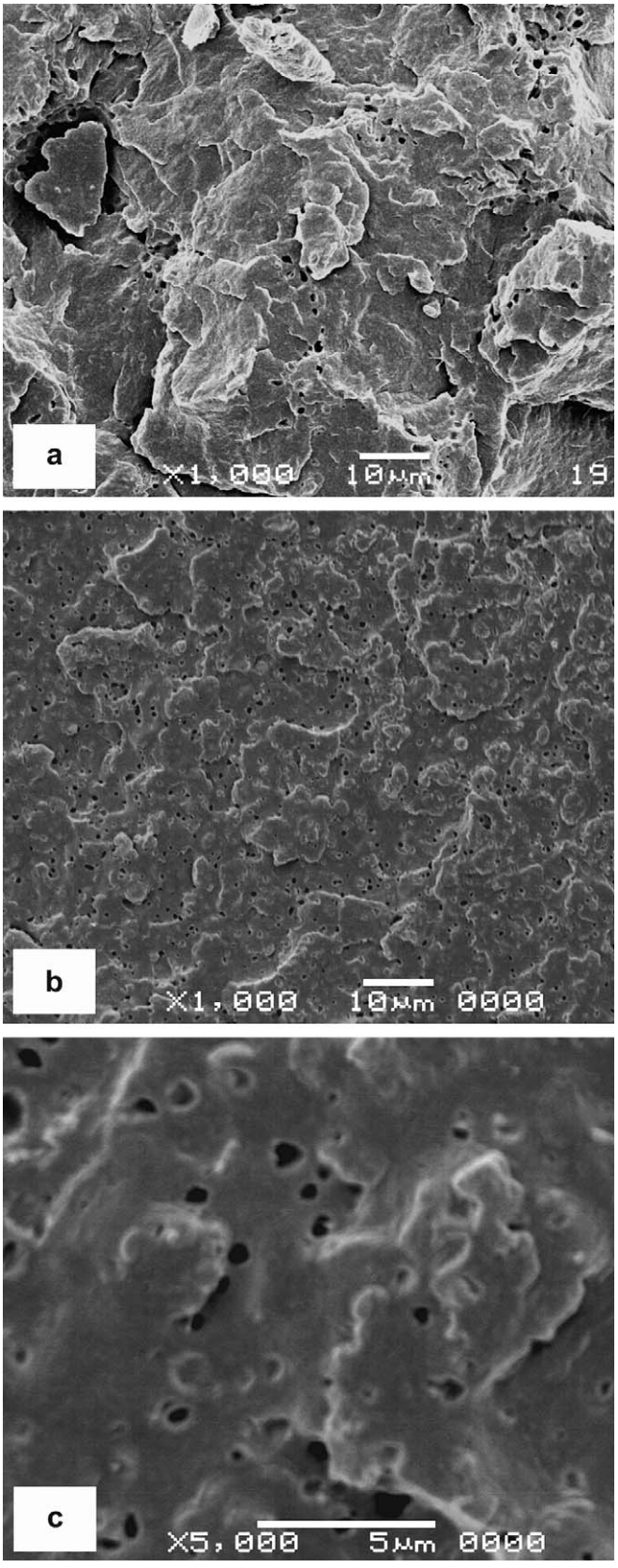

Fig. 8. SEM micrographs of fracture surfaces of blends: PLA/PPG1-5 (a) and PLA/PPG1-10 (b,c).

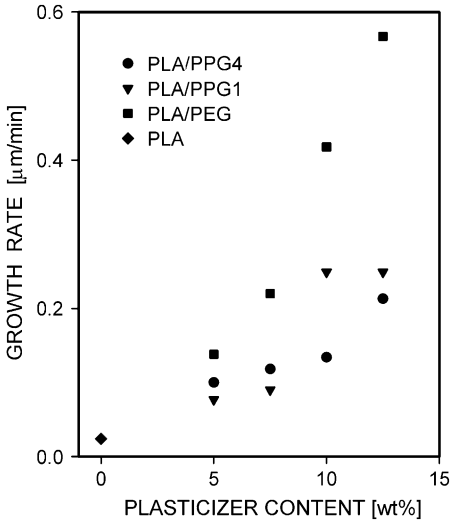

Fig. 9. Spherulite growth rate at 90 °C in neat PLA and in PLA/PPG4, PLA/PPG1, PLA/PEG blends vs. plasticizer content.

The acceleration of the growth indicates that plasticizer concentration at the crystallization front increased during crystallization. The effect was less pronounced in PLA/PPG blends although the growth in those blends was slower and the nucleation was weaker than that in PLA/PEG blends leaving more time for rejection of plasticizer molecules to a polymer melt at growing faces of spherulites.

3.2. Tensile behaviour

Exemplary stress–strain dependencies for the materials studied are plotted in Fig. 11. Neat PLA yielded at the deformation of about 5% and the stress above 50 MPa and exhibited low ability to plastic flow; the average elongation and the

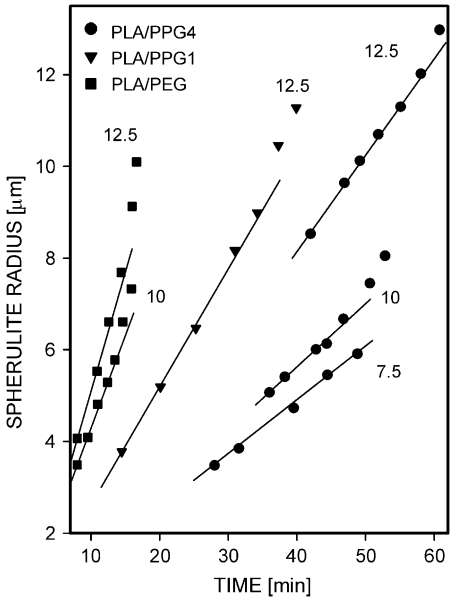

Fig. 10. Exemplary dependencies of a spherulite radius on time in plasticized PLA.

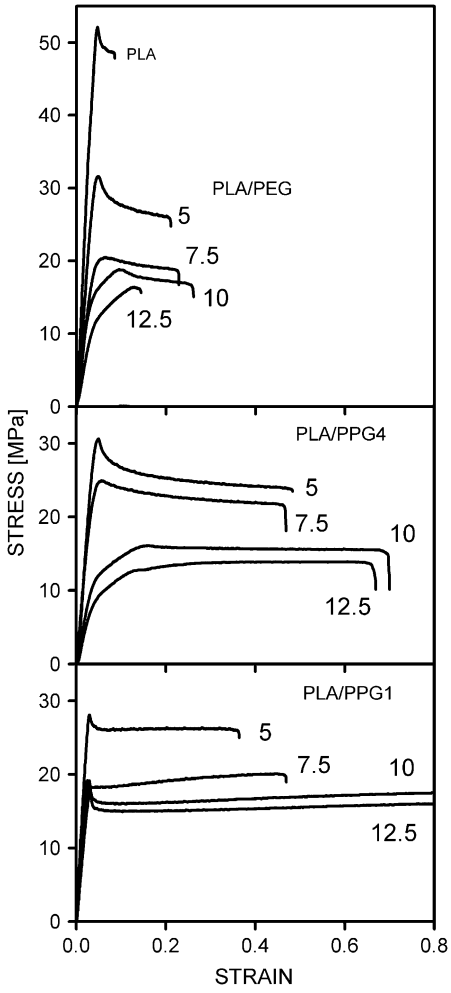

Fig. 11. Stress–strain plots for neat PLA, PLA/PPG4, PLA/PPG1 and PLA/PEG blends. Plasticizer content indicated in the figure.

stress at break were about 8% and 46 MPa, respectively. The plasticizers caused a decrease of the yield stress in all the blends and an increase of the elongation at break. The stress at break lowered for all materials with the increase of plasticizer content plasticizer content. Average values of elongation and stress at break of the blends are listed in Table 1.

A pronounced yield was observed for all the PLA/PPG1 blends; at the stress decreasing with the increase of PPG1 content from approx. 30 MPa to values below 20 MPa. In the PLA/PPG1 blends a strain to fracture increased gradually up to about 100%. The other blends exhibited a pronounced yield only for low contents of plasticizers; at 31 and 20 MPa for 5 and 7.5 wt% of PEG, and at 30 and 25.5 MPa for 5 and 7.5 wt% of PPG4, respectively. PLA/PEG-10, PLA/PEG-12.5, PLA/PPG4-10 and PLA/PPG4-12.5 behaved differently. The stress–strain dependencies deviated from linearity at a relatively small stress: 15 and 11 MPa for 10 and 12.5 wt% of PEG, while 11 and 8 MPa for 10 and 12.5 wt% of PPG4, respectively. The stress increased further until maximum value, then dropped and leveled off. With the increase of PEG content up to 10 wt% the elongation at break reached 26%, but the higher content of PEG, 12.5 wt%, resulted in shorter elongation, of approx. 15%. Larger elongations to break were achieved for PLA/PPG blends. The increase of PPG4 content to 10 wt% resulted in an increase of elongation to 65%; for PLA/PPG4-12.5 blend the similar elongation was achieved.

Table 1
Average stress at break, σ, and elongation at break, ε, of PLA/PPG4, PLA/PPG1 and PLA/PEG blends

Plasticizer content (wt%)	PLA/PPG4		PLA/PPG1		PLA/PEG	
	σ (MPa)	ε (m/m)	σ (MPa)	ε (m/m)	σ (MPa)	ε (m/m)
5	23.5	0.40	23.9	0.35	25.5	0.20
7.5	20.4	0.40	18.9	0.45	18.0	0.25
10	14.6	0.65	15.8	0.90	17.1	0.25
12.5	12.9	0.65	15.1	1.05	15.8	0.15

The gauge regions of all the specimens stress-whitened. The light microscopy observation with polarizers rotated by 45° with respect to the drawing direction revealed in neat PLA craze-like long fissures, perpendicular to the drawing direction (Fig. 12). In the blends structural features are very dense and recognizable only in less deformed regions of the gauge. In all PLA/PPG4 blends fissures along interspherulitic boundaries were observed in tensile specimens, as shown in Fig. 13. The effect intensified with increasing plasticizer content. Similar fissures were seen in PLA/PEG blends with higher PEG contents. In specimens of PLA/PPG1-5 and PLA/PPG1-7.5 dark branched bands essentially normal to the drawing direction, were composed from black rounded entities, of approx. 1–3 μm in diameter. In contrast, in PLA/PPG1-10 and PLA/PPG1-12.5 rather straight dark fissures appeared with discrete structure indiscernible by light microscopy.

The SEM micrographs revealed rather brittle fracture of PLA with little amount of plastic deformation (Fig. 14). An increase of the plasticizer content resulted in a larger amount of plastically deformed polymer on fracture surfaces. Patterns of hollows surrounded by plastically deformed walls were distinguishable on fracture surfaces of all PLA/PPG4 (Fig. 15) and PLA/PEG (Fig. 16) tensile specimens. Dimple patterns found

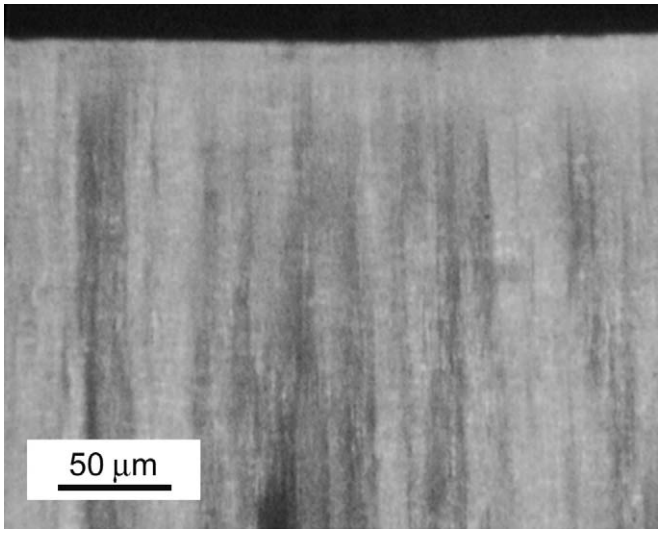

Fig. 12. Polarized light micrographs of the gauge region of neat PLA. Horizontal drawing direction.

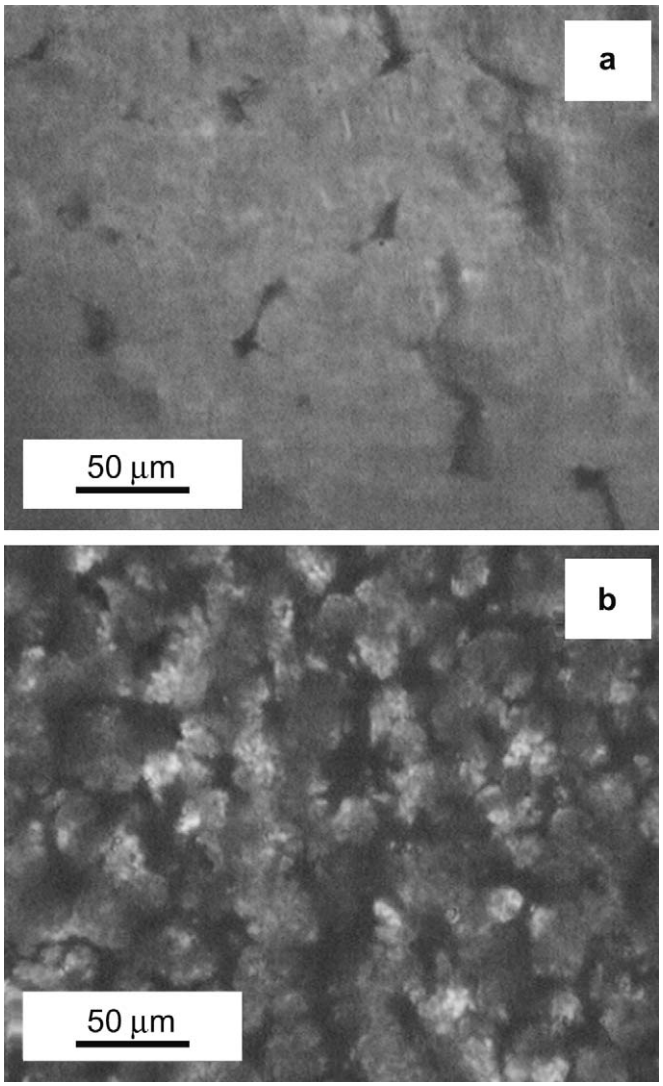

Fig. 13. Polarized light micrographs of deformed PLA/PPG4-5 (a) and PLA/PPG4-12.5 (b).

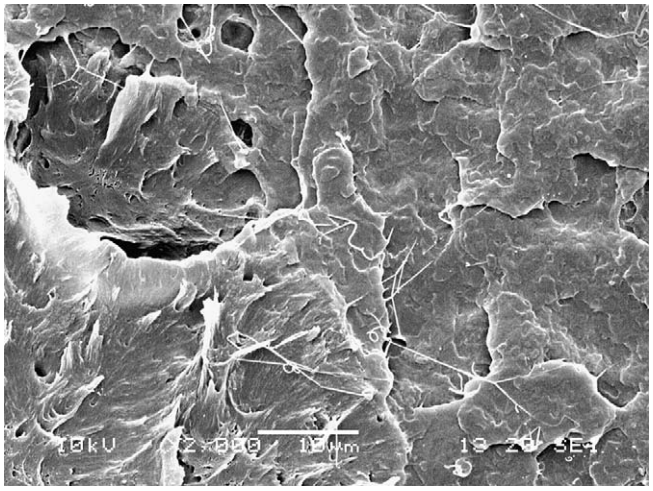

Fig. 14. SEM micrographs of surface of fractured tensile specimen of neat PLA.

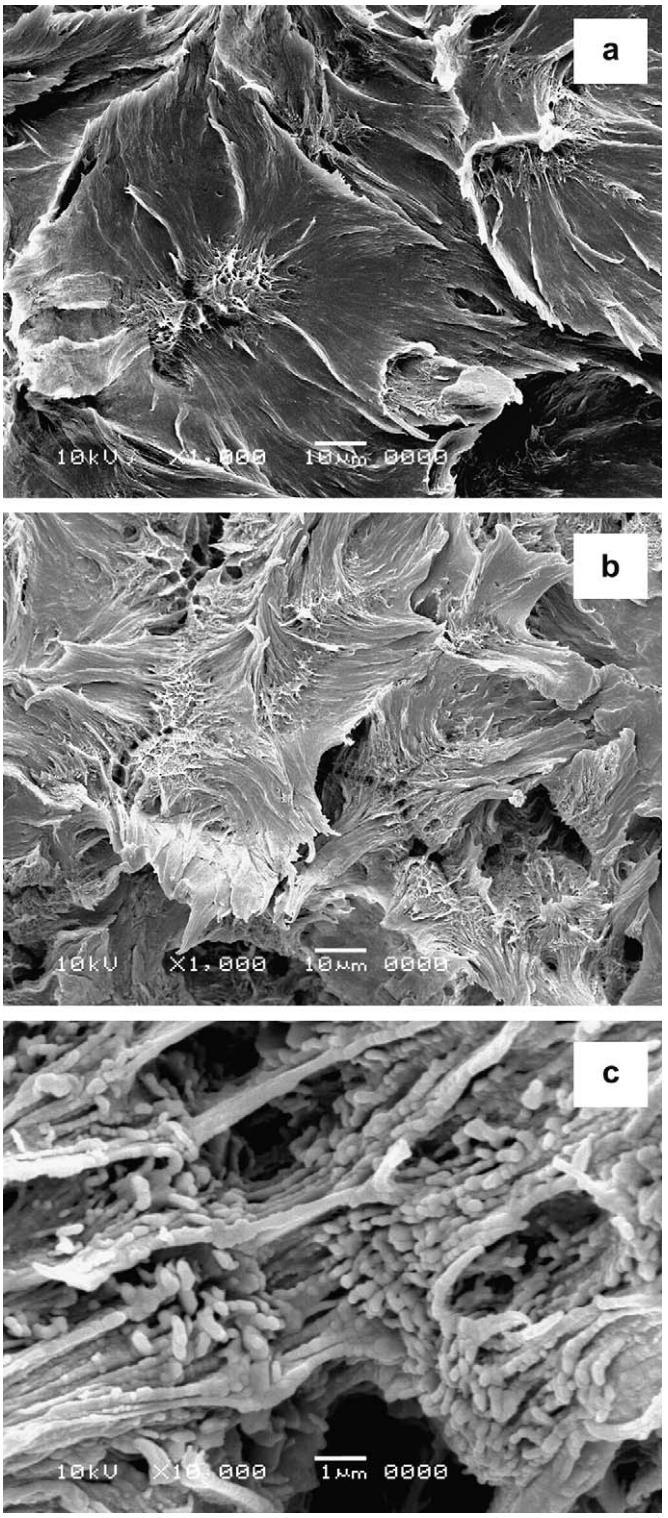

Fig. 15. SEM micrographs of surface of fractured tensile specimen of PLA/PPG4-7.5 (a), PLA/PPG4-12.5: overview (b) and detail (c).

on fracture surfaces of other semicrystalline polymers are attributed to straining craze fibrils to fracture [27]. The walls surrounding hollowed cells were usually more deformed in samples with higher plasticizer content. In PLA/PPG4 blends central parts of some of these hollows exhibited crazes developed along interspherulitic boundaries. Such a picture

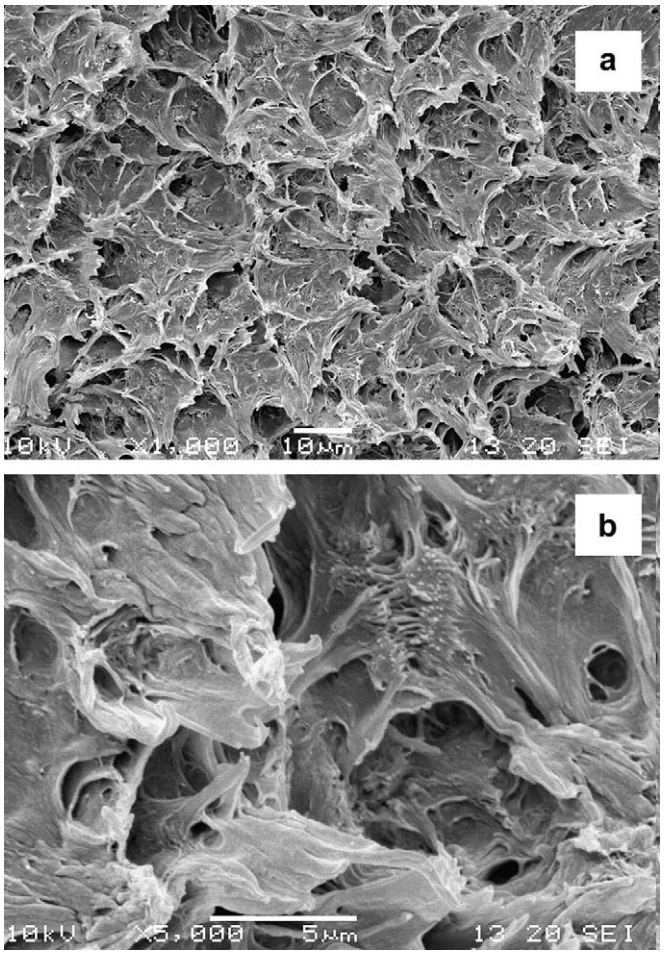

Fig. 16. SEM micrographs of surface of fractured tensile specimen of PLA/PEG-12.5; overview (a) and detail (b).

conforms to the features found by polarized light microscopy. Separation of the plasticized material along interspherulitic boundaries, seen by light microscopy, was also recognizable on SEM micrographs of tensile specimens of PLA/PEG blends although less clearly than in PLA/PPG4 samples which were more strained and contained larger spherulites. On PLA/PPG1-5 fracture surface the plastic deformation was concentrated in walls between pools of phase separated plasticizer, while the pool-free areas fractured in a brittle manner, as it is shown in Fig. 17a. The pool size, about 0.5–3 μm, conforms to the sizes of rounded entities resolved by light microscopy. Increase of PPG1 content resulted in an increased amount of plastically deformed material forming a pattern bearing some resemblance to the dimple pattern typical of other blends (Fig. 17b and c). However, on fracture surface of PLA/PPG1-10 and PLA/PPG-12.5 the dominant features are deformed walls of drawn polymer surrounding deep hollows of relatively small, 1–3 μm, size.

4. Discussion and conclusions

All the blends exhibited the ability to plastic deformation higher than that of neat PLA, due to plasticization of their

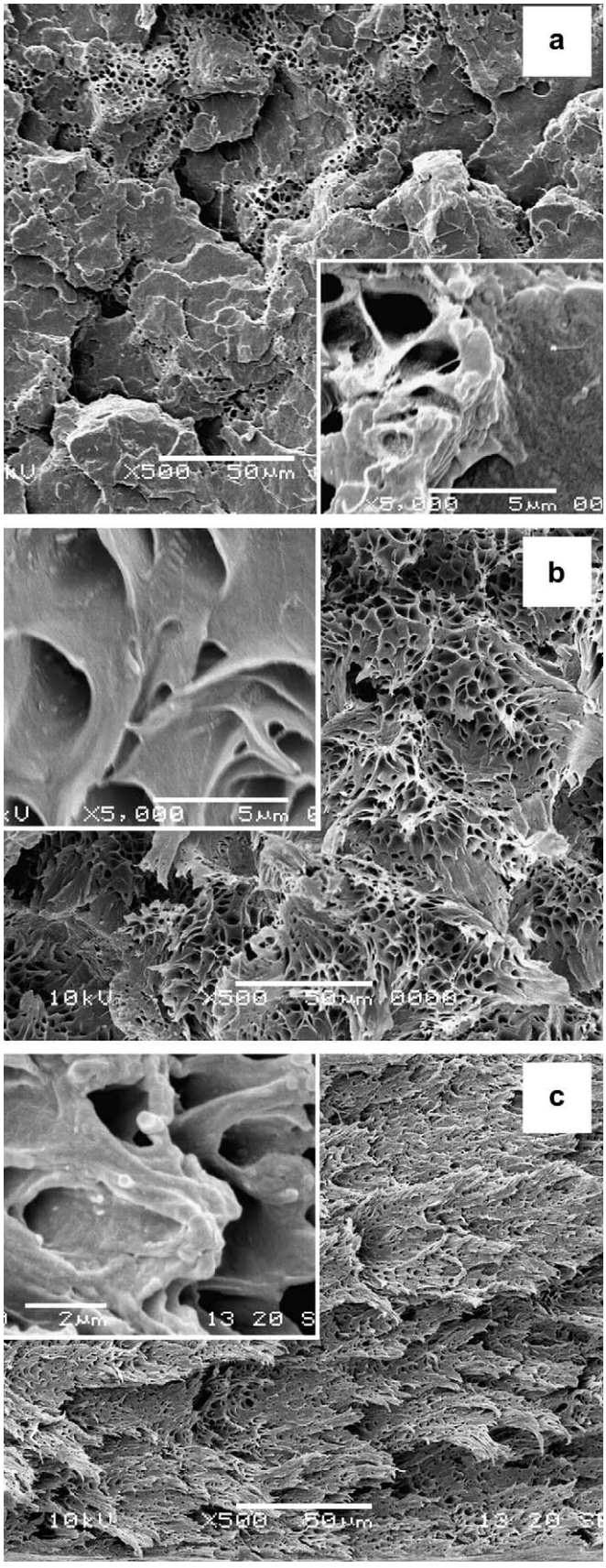

Fig. 17. SEM micrographs of surface of fractured tensile specimen of PLA/PPG1-5 (a), PLA/PPG1-7.5 (b), PLA/PPG1-10 (c).

amorphous phase. Yield stress lowered in all the blends with the increase of plasticizer content indicating easier onset of plastic deformation. We note that a crystallinity level of PLA and a long period were similar in all the materials studied. In all the blends, except for PLA/PEG-5 a phase separation occurred during crystallization. In neat and plasticized PLA crazes were evidenced by SEM and/or light microscopy; similarly as described in Ref. [10]. It was established in the past that a low crystallinity level and fine spherulitic structure, like in the materials studied, were advantageous for development of crazes in the semicrystalline polymers.

The PLA/PPG4 and PLA/PEG blends revealed many similarities. In both cases the increase of plasticizer content from 7.5 to 10 wt% resulted in a significant change of stress–strain dependence. A departure of stress–strain dependence from linearity occurred at low strain while a pronounced yield, visible for lower contents of plasticizer disappeared. The increase of the plasticizer content from 10 to 12.5 wt% decreased slightly the flow stress but the elongation at break did not increase.

The interspherulitic boundaries are the weakest elements of a spherulitic structure in both types of the blends. The cracks preferentially propagated through interspherulitic crazes. It is known that the weakness of the boundaries derives from slow crystallization process, when additives, impurities, low molecular weight polymer and non-crystallizable chains are partly rejected from spherulites and accumulated at the growth fronts [27]. In plasticized PLA, the concentration of plasticizer has to increase in the amorphous phase during crystallization, at average approx. by 50% of its initial value. However, depending on the diffusion mobility of non-crystallizable molecules, interfacial tension and time-scale of crystallization, the molecules can either be entrapped within interlamellar regions or diffused in radial direction toward the molten polymer [28]. In the last case an accumulation of non-crystallizable additives induces a change in the spherulite growth rate [29].

The acceleration of spherulite growth rate observed for PLA/PPG4 and PLA/PEG blends with 10 and 12.5 wt% of plasticizer evidenced that plasticizer content in the vicinity of crystallizing front was increasing during crystallization. The broadening of high temperature $\log E''$ peaks recorded for these blends is suggestive of plasticizer concentration gradient. The DSC and DMTA measurements supported a phase separation in both types of blends, especially in the samples with high plasticizer content, that was caused by a redistribution of the plasticizer during crystallization. We note that a phase separation may occur also within spherulites in confined amorphous layers approx. 14 nm thick, between lamellae, however, this might be obstructed by bonding of PLA amorphous phase to crystalline phase and by geometrical restrictions for diffusion and coalescence.

The boundaries between adjacent spherulites are crossed by short end sections of lamellae and eventually by some interspherulitic links. Stronger are the amorphous intersections between radially extended lamellae which are fortified by interlamellar tie molecules. While a plasticizer, confined in the amorphous phase essentially increases the ability of this phase to plastic flow, it also worsens a linkage between adjacent lamellae within the same spherulite and neighboring spherulites. Thus, the abundance of relatively short plasticizer macromolecules accumulated within interspherulitic boundaries may rather worsen than improve ultimate properties of a blend. This explains why a decrease of yield and flow stresses was not followed by larger elongation at break when the plasticizer concentration increased from 10 to 12.5 wt%. However, while the elongation was the same for the PLA/PPG4-10 and PLA/PPG4-12.5 in PLA/PEG blends it decreased drastically when PEG content exceeded 10 wt%. The acceleration of the spherulite growth rate can serve as a measure of the increase of plasticizer concentration in front of a growing spherulite. Considering the dependence of the initial G value on plasticizer content one finds that plasticizer concentration in front of a growing spherulite at least doubled in PLA/EG-12.5, while in other cases it increased considerably less, approx. by one-third of the initial value. This explains the weakness of interspherulitic boundaries in the PLA/PEG-12.5 and the smallest elongation at break measured for this material. PPG4 molecules with CH_3 side groups are more likely to remain entrapped within interlamellar amorphous layers than linear PEG of the same molecular weight.

The PLA/PPG1 blends behaved differently in tensile tests than PLA/PPG4 and PLA/PEG blends. The pronounced yield was visible for all compositions studied. With the increase of PPG1 content a yield stress and flow stress decreased while the elongation at break increased. Separation of PPG1 was evidenced by SEM and also observed by DMTA and DSC techniques. The increase of $\log E''$ glass transition peak temperature after crystallization in all the PLA/PPG1 blends, by 3.5–7.5 K, shows that the plasticizer concentration in PLA rich phase is lower than that in the amorphous blends with the same composition.

In PLA/PPG1-5 the emptied pools were concentrated in narrow zones, at interspherulitic boundaries and at spherulite peripheries. With the increase of PPG1 content the zones containing the pools broadened; in the samples of PLA/PPG1-10 and PLA/PPG1-12.5 a uniform distribution of emptied pools was observed. These two blends exhibited similar T_g and G, and also similar behaviour in tensile experiments, breaking at the relatively low stress of 15–16 MPa and elongation of about 100%. The $\log E''$ glass transition peaks did not broaden with the increase of PPG1 content indicating that the plasticizer concentration gradient did not build up. The spherulite growth rate was most stable in the PLA/PPG1 blends. Acceleration of the growth rate in the blend PLA/PPG1-12.5, from 0.25 to 0.32 μ/min, recorded at the end of crystallization, indicated the increase of PPG1 concentration in front of spherulite only by approx. 10% of its initial value, as it can be judged from the growth rate dependence on the initial PPG1 content. The stability of PPG1 concentration in PLA rich phase was obviously facilitated not only by larger molecular weight of this plasticizer, preventing it from diffusion from interlamellar regions to polymer melt surrounding spherulites, but also by the phase separation that resulted in relatively high T_g values of the PLA rich phase. The phase separation in PLA/PPG1-12.5 blend occurred even before the crystallization [14] although the crystallization augmented the process. The plastic deformation

of PLA/PPG1 blend was in a form of walls of plastically deformed material surrounding deep hollows of size of 1–3 μm. The fracture surfaces of the PLA/PPG1-10 and PLA/PPG1-12.5 blends exhibited the most uniform distribution of plastically deformed material and exhibited the best drawability.

The effect of local plasticization by droplets of low molecular weight polybutadiene, advantageous for advancement of crazes in glassy polystyrene, was observed in the past [30]. The structure of fracture surfaces is suggestive of strong deformation of a polymer between the liquid inclusions. Thus, the local plasticization mechanism seems to act in the case of PLA/PPG1 blends, especially with high PPG1 content, where PPG1 inclusions are uniformly distributed across a sample. This could counteract the relatively high T_g values of the PLA rich phase in the PLA/PPG1 blends that was another effect of the phase separation.

It is obvious that to facilitate the plastic deformation of semicrystalline polymer, with glassy amorphous phase, the plasticization of the latter and sufficient decrease of T_g are required. However, crystallization while increasing the average plasticizer content in the amorphous phase may also induce a rejection of plasticizer from growing spherulites and its accumulation at interspherulitic boundaries. Local excessive amount of a plasticizer can weaken the links between lamellae and also between neighboring spherulites that caused premature failure of the material. The molecular architecture and molecular weight of polymeric plasticizer are therefore crucial. An increase of plasticizer molecular weight will slow down the diffusion of plasticizer from the interlamellar amorphous phase to polymer melt in front of growing spherulites and accumulation within interspherulitic boundaries but would require also an increase of its concentration. Too high amount of a plasticizer will not assure the proper linkage between lamellae and between spherulites. In the paper we have demonstrated that the negative aspects of plasticization of semicrystalline PLA can be reduced by using PPG instead of PEG.

Although not investigated in the present paper, crystallinity level, nucleation intensity and spherulite growth rate related to D-lactide content and crystallization conditions may have an important effect on the properties of crystallized plasticized PLA, as they control a build up of plasticizer gradient.

The increase of plasticizer content or/and annealing of the blends at crystallization temperature can induce a phase separation depleting the PLA rich phase of plasticizer. However, the tiny pools of liquid plasticizer obviously enhance the plastic deformation. Thus, while solid inclusions of crystallizable plasticizers like PEG are undesirable as they degrade the blend drawability, tiny pools of liquids, like PPG, may locally plasticize PLA during deformation and have a positive effect on drawability.

Acknowledgments

This work was partially supported by the Ministry of Science and Society Information Technologies (Poland) through the Centre of Molecular and Macromolecular Studies, PAS, under Grant PBZ KBN 070/T09/2001, 2003–2006.

References

[1] Perego G, Cella GD, Bastioli C. J Appl Polym Sci 1996;59:37.
[2] Bechtold K, Hillmyer MA, Tolman WB. Macromolecules 2001;34:8641.
[3] Nijenhuis AJ, Colstee E, Grijpma DW, Pennings AJ. Polymer 1996;37:5849.
[4] Labrecque LV, Kumar RA, Dave V, Gross RA, McCarthy SP. J Appl Polym Sci 1997;66:1507.
[5] Ljungberg N, Wesselen B. J Appl Polym Sci 2002;86:1227.
[6] Jacobsen S, Fritz HG. Polym Eng Sci 1999;39:1303.
[7] Martin O, Averous L. Polymer 2001;42:6209.
[8] Baiardo M, Frisoni G, Scandola M, Rimelen M, Lips D, Ruffieux K, et al. J Appl Polym Sci 2003;90:1731.
[9] Hu Y, Rogunova M, Topolkaraev V, Hiltner A, Baer E. Polymer 2003; 44:5701.
[10] Kulinski Z, Piorkowska E. Polymer 2005;46:10290.
[11] Hu Y, Hu YS, Topolkaraev V, Hiltner A, Baer E. Polymer 2003;44:5711.
[12] Sheth M, Kumar RA, Dave V, Gross AR, McCarthy SP. J Appl Polym Sci 1997;66:1495.
[13] Pluta M, Paul MA, Alexandre M, Dubois Ph. J Polym Sci Part B Polym Phys 2006;44:312.
[14] Kulinski Z, Piorkowska E, Gadzinowska K, Stasiak M. Biomacromolecules, in press, doi: 10.1021/bm060089m.
[15] Tsuji H, Ikada Y. Macromol Chem Phys 1996;197:3483.
[16] Kuran W. In: Salamone JC, editor. Concise polymeric materials encyclopedia. Boca Raton, London, New York, Washington: CRS Press; 1999. p. 1278–9.
[17] Pluta M, Galeski A. J Appl Polym Sci 2002;86:1386.
[18] Bailey Jr FE, Koleske JV. Poly(ethylene oxide). New York: Academic Press; 1976. p. 23.
[19] Bates FS, Cohen RE, Argon AS. Macromolecules 1983;16:1108.
[20] Piorkowska E, Galeski A. J Polym Sci Part B Polym Phys 1993;31:1285.
[21] DeSantis P, Kovacs A. Biopolymers 1968;6:299.
[22] Miyata T, Masuko T. Polymer 1997;38:4003.
[23] Sarasua JR, Prud'homme RE, Wisniewski M, Le Borgne A, Spassky N. Macromolecules 1998;31:3895.
[24] Lai WCh, Liau WB, Lin TT. Polymer 2004;45:3073.
[25] Chartoff RP. In: Turi EA, editor. Thermal characterization of polymeric materials, vol. 1. San Diego: Academic Press; 1997. p. 484–743.
[26] Pluta M, Paul MA, Alexandre M, Dubois Ph. J Polym Sci Part B Polym Phys 2006;44:299.
[27] Friedrich K. Adv Polym Sci 1983;52/53:225.
[28] Keith HD, Padden Jr FJ. J Appl Phys 1964;35:1270.
[29] Bartczak Z, Galeski A, Martuscelli E. Polym Eng Sci 1984;24:1155.
[30] Argon AS, Cohen RE. Adv Polym Sci 1990;91/92:301.